

Regular article

Ab initio molecular orbital study of $\text{Fe}(\text{CO})_n$ ($n = 1-3$)

Hiroaki Honda¹, Takeshi Noro¹, Eisaku Miyoshi²

¹Division of Chemistry, Graduate School of Science, Hokkaido University, Sapporo 060-0810, Japan

²Institute for Molecular Science, Myodaiji, Okazaki 444-8525, Japan

Received: 27 September 1999 / Accepted: 13 January 2000 / Published online: 19 April 2000

© Springer-Verlag 2000

Abstract. Geometry optimization was performed for the ground states of FeCO , $\text{Fe}(\text{CO})_2$, and $\text{Fe}(\text{CO})_3$ at various levels of ab initio calculations, and the bond lengths and dissociation energies obtained were in reasonable agreement with experimental results. The nature of bonding was studied for these molecules using a complete-active-space self-consistent-field method. From the Mulliken population analysis, it was found that the traditional donation and back donation mechanism is valid for these molecules, including $\text{Fe}(\text{CO})_3$, which has a pyramidal structure.

Key words: Nature of bonding for $\text{Fe}(\text{CO})_n$ ($n = 1-3$) – Complete-active-space self-consistent-field method – Multireference configuration interaction – Mulliken population analysis – Charge density difference map

1 Introduction

Various unsaturated iron carbonyl complexes, $\text{Fe}(\text{CO})_n$ ($n = 1-4$), have been produced by the UV photolysis of iron pentacarbonyl, $\text{Fe}(\text{CO})_5$ [1]. Among them, the FeCO radical has been extensively investigated in spectroscopic studies performed from both experimental [1–11] and theoretical [12–19] points of view.

Villalta and Leopold [8] showed from their vibrationally resolved photodetachment spectra that the ground state of FeCO is the $^3\Sigma^-$ state and that the $^5\Sigma^-$ state is located only $1135 \pm 25 \text{ cm}^{-1}$ above the ground state. The vibrational frequencies of the C–O stretching and Fe–C stretching modes in the ground state were observed at 1950 ± 10 and $530 \pm 10 \text{ cm}^{-1}$, respectively. These authors also determined that the dissociation energy of FeCO was $0.46 \pm 0.16 \text{ eV}$. From the rotational spectra of FeCO , Kasai et al. [9] derived Fe–C and C–O bond lengths of 1.7268 and 1.15987 Å, respectively. Recently, Tanaka et al. [10] analyzed the C–O stretch-

ing band of FeCO using rotationally resolved IR diode laser spectroscopy [1] and millimeter-wave spectroscopy [10] and provided direct experimental evidence that the ground state of FeCO has $^3\Sigma^-$ symmetry. These authors determined the C–O band origin to be $1946.47060 \text{ cm}^{-1}$ and the Fe–C and C–O bond lengths to be 1.7270 and 1.1586 Å respectively.

Tanaka and coworkers [1, 11] reported that the $\text{Fe}(\text{CO})_2$ radical has a $^3\Sigma_g^-$ electronic ground state with $D_{\infty h}$ symmetry and that the vibrational frequency of the C–O antisymmetric stretch is located at $1928.184335 \text{ cm}^{-1}$. The vibrational frequency is lower than that of the C–O stretch of FeCO by only 18 cm^{-1} . This shows that the difference in C–O bonding nature is small between the FeCO and $\text{Fe}(\text{CO})_2$ radicals. They also calculated the Fe–C length to be 1.7979 Å from the observed rotational constant under the assumption of a fixed C–O length of 1.156 Å.

Kasai estimated the Fe–C bond length of $\text{Fe}(\text{CO})_3$ (the 3A_2 ground state in C_{3v} symmetry) as 1.965 Å from observed rotational constants under the assumption of a fixed C–O length of 1.156 Å.

Various levels of calculations [12–24] have been performed to calculate the spectroscopic constants of $\text{Fe}(\text{CO})_n$ ($n = 1-3$). In two such studies, Adamo and Leij [18, 19] performed the natural bond analysis for FeCO at a density functional level. Their results strongly support the traditional picture of a metal carbonyl bond, as characterized by both donation and back donation contributions. The nature of the bonding was also investigated by Bauschlicher et al. [12], who analyzed complete-active-space self-consistent-field (CASSCF) wave functions using the constrained space variation technique and found that the metal-to-CO π back donation made the largest interunit contribution to the bonding and that the electronic correlation increased the importance of this effect. Extensive calculations were performed on $\text{Fe}(\text{CO})_n$ ($n = 1-5$) by Barnes et al. [22] using the modified coupled-pair functional (MCPF) method. Their main interest was the determination of all the dissociation energies for individual fragments. They were also interested in accurate geometries and force constants of $\text{Fe}(\text{CO})_n$ fragments. Although there have

been several other theoretical studies on $\text{Fe}(\text{CO})_2$ and $\text{Fe}(\text{CO})_3$ [20–24], there have been few comprehensive studies on the change in bonding nature in the $\text{Fe}(\text{CO})_n$ ($n = 1-3$) radicals.

Our present interest is the nature of the bonding in $\text{Fe}(\text{CO})_n$ with respect to changes in the number of CO ligands. We will investigate spectroscopic constants of the $\text{Fe}(\text{CO})_n$ ($n = 1-3$) radicals by the use of ab initio calculations and discuss the change in the bonding nature through the donation and back donation scheme in the radicals.

2 Method of calculation

2.1 Basis set

For Fe, minimal basis functions corresponding to the $1s-3s, 2p$, and $3p$ orbitals were taken from the (843/84) set of Koga et al. [25], while the $4s$ and $3d$ functions and polarization functions were taken from a double zeta valence set and the $[2p1d1f]$ set which were recently developed by Noro et al. These contraction coefficients and orbital exponents were determined by minimizing the difference from an average of accurate atomic natural orbitals for the $4s^2 3d^6$ and $4s^1 3d^7$ atomic states. The C and O basis sets used were the $(7s4p/7s4p)/[3s2p/3s2p]$ Gaussian sets of Huzinaga et al. [26] augmented by the $(2d/2d)/[1d/1d]$ polarization functions [27]. The present basis sets gave 1.109 and 1.123 Å for the internuclear distance of CO at the SCF and single and double excitation configuration interaction (SDCI) levels, respectively. These results are in reasonable agreement with the experimental value of 1.1281 Å [28].

2.2 CASSCF–SDCI calculations

We carried out CASSCF CI calculations. The states considered in this study were the ground states of three molecules, namely $^3\Sigma^-$, $^3\Sigma_g^-$, and 3A_2 for FeCO , $\text{Fe}(\text{CO})_2$ and $\text{Fe}(\text{CO})_3$, respectively. The active orbitals of the CASSCF calculations consisted of molecular orbitals arising from $3d$ and $4s$ of Fe and $2\pi^*$ of each CO ligand, where the eight electrons in the $3d$ and $4s$ orbitals of the Fe atom were correlated. The numbers of configuration state functions thus generated were 600, 5220, and 56728 for FeCO , $\text{Fe}(\text{CO})_2$, and $\text{Fe}(\text{CO})_3$, respectively. For FeCO , we performed an extended CASSCF, in which we added 5σ and 1π of the CO ligand to the active space.

SDCI calculations from the Hartree–Fock configuration were performed for each molecule. We considered correlation effects among $4s$ and $3d$ electrons of Fe and 1π and 5σ electrons of CO. Furthermore, we carried out multireference SDCI (MRSDCI) for FeCO and $\text{Fe}(\text{CO})_2$. As reference functions, we chose configurations with coefficients larger than 0.1 in the CASSCF wave functions. The dimensions of the MRSDCI were 818,209 and 3,390,345 for FeCO and $\text{Fe}(\text{CO})_2$, respectively. Unfortunately, we could not perform the same level of the calculation for $\text{Fe}(\text{CO})_3$ due to the computer resource we used.

At each level of the calculations described previously, we optimized the Fe–C and C–O bond lengths for three molecules, with the constraints of linear structures for FeCO and $\text{Fe}(\text{CO})_2$ and C_{3v} symmetry and Fe–C–O bond angles of 180.0° for $\text{Fe}(\text{CO})_3$. At the CASSCF level, we calculated the dissociation energies per CO ligand by using the following formula:

$$DE_0 = E_{\text{opt}}[\text{Fe}(\text{CO})_{n-1}] + E_{\text{opt}}[\text{CO}] - E_{\text{opt}}[\text{Fe}(\text{CO})_n],$$

where E_{opt} represents the total energy calculated at the optimized geometry. For FeCO ($n = 1$), the dissociation energy is calculated with respect to the SCF energies of the ground states of Fe and CO.

All calculations were performed on an IBM/RS6000 system using the ALCHEMY II program [29, 30].

3 Results and discussion

3.1 Optimized geometries

The optimized geometries and dissociation energies are shown in Table 1 along with previous theoretical and experimental results. We first consider the results for FeCO . At the CASSCF levels, we obtained $R(\text{Fe}-\text{C})$ of 1.785–1.795 Å, approximately 0.06–0.07 Å larger than the experimental value. Inclusion of correlation effects gave $R(\text{Fe}-\text{C})$ of 1.672 and 1.757 Å at the SDCI and MRSDCI levels, respectively, which deviated from the experimental value by 0.055–0.030 Å. The small CASSCF and SDCI produced $R(\text{C}-\text{O})$ of 1.132 and 1.134 Å, respectively, which are slightly smaller than the experimental value of 1.159 Å. Inclusion of 1π in the active space in the CASSCF and $1\pi^2 \rightarrow 2\pi^{*2}$ in the reference space in the CI reduced these errors and yielded $R(\text{C}-\text{O})$ s of 1.150 and 1.155 Å for larger CASSCF and MRSDCI, respectively. MCPF results by Barnes et al. [22] gave excellent agreement for $R(\text{Fe}-\text{C})$, but yielded a considerable discrepancy of 0.050 Å for $R(\text{C}-\text{O})$. They used a triple zeta basis set for Fe, C, and O, but did not employ polarization functions. When we remove the polarization functions from our basis set, the internuclear distance of the CO molecule increases by 0.040 Å. Thus, the present SDCI and MRSDCI calculations gave better agreement with the experimental

Table 1. Summary of $\text{Fe}(\text{CO})_n$ ($n = 1-3$) results. The bond lengths are in Angstroms, the bond angle is in degrees, and the dissociation energy (DE) is in kilocalories per mole. The data in parentheses are dissociation energies corrected using the experimental excitation energy of 3F of Fe

Method	$R(\text{Fe}-\text{C})$	$R(\text{C}-\text{O})$	$\angle(\text{C}-\text{Fe}-\text{C})$	DE
FeCO				
CASSCF	1.795	1.132		–10.9 (12)
Large CASSCF	1.785	1.150		
SDCI	1.672	1.134		
MRSDCI	1.757	1.155		
MCPF ^a	1.720	1.209		–9.8 (5)
Expt.	1.727 ^b	1.159 ^b		8.1 ± 3.5^f
Fe(CO)₂				
CASSCF	1.889	1.118		20.3
SDCI	1.826	1.122		
MRSDCI	1.848	1.127		
MCPF ^a	1.918	1.173		22
Expt.	1.7979 ^c	1.1586 ^c		36.7 ± 3.5^f
Fe(CO)₃				
CASSCF	1.925	1.125	105.5	39.6
SDCI	1.888	1.127	104.8	
MCPF ^a	1.905	1.180	108.0	25
Expt.	1.965 ^d	1.156 ^d	108 ± 3^e	29.1 ± 3.5^f

^a Ref. [22]

^b Ref. [10]

^c Ref. [11]. The C–O bond length was assumed to be the same as in FeCO

^d The C–O bond length was assumed to be the average of the value of FeCO and $\text{Fe}(\text{CO})_2$

^e Ref. [33]

^f Ref. [3]

values for $R(\text{Fe}-\text{C})$ and $R(\text{C}-\text{O})$ than the previous MCPF calculation did.

For the dissociation energy, we obtained a negative value of -10.9 kcal/mol at the CASSCF level. The $^3\Sigma^-$ state has the ^3F state of Fe as the asymptote. At the SCF level, the ^3F state is calculated to be 22.8 kcal/mol too high in energy compared to the ^5D ground state because the different occupation number of the $3d$ shell causes large differential correlation effects. Thus, when we calculated the dissociation energy relative to the ^3F state and used the experimental separation, the dissociation energy became 12 kcal/mol, a value very close to the experimental value of 8.1 ± 3.5 kcal/mol.

For $\text{Fe}(\text{CO})_2$, $R(\text{Fe}-\text{C})$ is longer by about 0.08 Å, while $R(\text{C}-\text{O})$ is shorter by about 0.04 Å compared with the experimental value [11] at the CASSCF level. Inclusion of the correlation effects reduced these errors to 0.03–0.05 Å for $R(\text{Fe}-\text{C})$ and 0.03 Å for $R(\text{C}-\text{O})$. On the other hand, the MCPF result [22] shows large discrepancy of 0.12 Å for $R(\text{Fe}-\text{C})$ due to the lack of polarization functions. The dissociation energy of CO for FeCO is 20 kcal/mol, a value close to that at the MCPF level, but 17 kcal/mol smaller than the experimental value.

For $\text{Fe}(\text{CO})_3$, $R(\text{Fe}-\text{C})$ is smaller than the experimental value by 0.04 Å at the CASSCF level. The SDCI result indicates that the inclusion of correlation effects further shortens the length. The calculated $R(\text{C}-\text{O})$ is smaller than the experimental value by about 0.03 Å at the CASSCF and SDCI levels. The calculated C–Fe–C angle is in good agreement with the experimental value. The total energy difference between $\text{Fe}(\text{CO})_3$ at C–Fe–C bond angles of 105.5° and 120.0° is only 0.6 kcal/mol; therefore, the potential-energy surface is shallow for the totally symmetric deformation in the umbrella motion. The dissociation energy of CO for $\text{Fe}(\text{CO})_2$ was calculated as 39.5 kcal/mol, which is larger than the experimental value of 29.1 and the MCPF result of 25 kcal/mol.

The resultant $R(\text{Fe}-\text{C})$ and $R(\text{C}-\text{O})$ for FeCO to $\text{Fe}(\text{CO})_3$ are shown in Fig. 1 along with the MCPF results. At all levels the present results show the same trend that $R(\text{Fe}-\text{C})$ increases monotonously in going from FeCO to $\text{Fe}(\text{CO})_3$; on the other hand, $R(\text{C}-\text{O})$ has a minimum at $\text{Fe}(\text{CO})_2$. Thus, we expect that the CASSCF wave functions are accurate enough to analyze the nature of the bonding in $\text{Fe}(\text{CO})_n$ with respect to changes in the number of CO ligands.

The frequencies were obtained by solving vibrational equations near equilibria using the VIBR4 program [31]. The vibrational frequencies of three molecules at the SDCI level are summarized in Table 2. For FeCO, the calculated frequencies of Fe–C and C–O stretches were 510.6 and 2058.2 cm^{-1} , respectively, which deviate from the experimental values by 20 and 110 cm^{-1} . We can compare the calculated frequency with the experimental one for the C–O antisymmetric stretch for $\text{Fe}(\text{CO})_2$, for which we obtained 2194.3 cm^{-1} , which is approximately 300 cm^{-1} higher than the experimental value. For $\text{Fe}(\text{CO})_3$, the calculated C–O totally symmetric stretch deviated from the experimental one by approximately

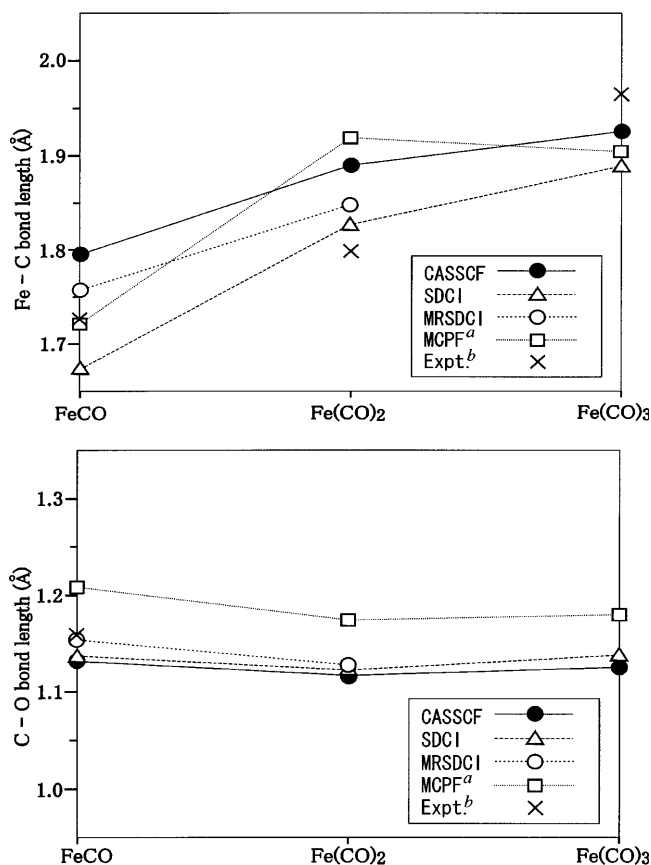


Fig. 1. Comparison of the theoretical and experimental Fe–C and C–O bond lengths for $\text{Fe}(\text{CO})_n$ ($n=1-3$)

Table 2. Vibrational frequencies (cm^{-1}) at the single and double excitation configuration interaction level

Method	Fe–C		C–O		
	ω_1^a	ω_2^b	ω_3^c	ω_4^d	ω_5^e
FeCO					
Present	510.6		2058.2		
Expt. ^f	530		1950		
Fe(CO) ₂					
Present	463.3	410.6	2328.9	2194.3	
Expt. ^g				1928.2	
Fe(CO) ₃					
Present	405.3		2325.9		1331.9
Expt. ^h			2042		

^a The Fe–C stretch for FeCO. The Fe–C totally symmetric stretch for $\text{Fe}(\text{CO})_2$ and $\text{Fe}(\text{CO})_3$. Ref. [22]

^b The Fe–C stretch for FeCO. The Fe–C antisymmetric stretch for $\text{Fe}(\text{CO})_2$. Ref. [10, 12]

^c The C–O stretch for FeCO. The C–O totally symmetric stretch for $\text{Fe}(\text{CO})_2$ and $\text{Fe}(\text{CO})_3$

^d The C–O antisymmetric stretch for $\text{Fe}(\text{CO})_2$

^e The totally symmetric deformation for $\text{Fe}(\text{CO})_3$

^f Ref. [8]

^g Ref. [11]

^h Ref. [34]

Table 3. Mulliken population of complete-active-space self-consistent-field (CASSCF) wave functions

	Donation ^a	Back donation ^b	Atomic orbital population			Net charge
			4s	4p	3d	
FeCO	0.476	0.530 (0.508) ^c	1.10	0.17	6.63	+0.10
Fe(CO) ₂	0.736	0.655 (0.579)	1.02	0.13	6.89	-0.04
Fe(CO) ₃	0.965	1.018 (0.956)	0.32	0.65	6.97	+0.06
<i>a</i> ₁	0.368	0.228				
<i>e</i>	0.597	0.785				
<i>a</i> ₂	–	0.005				

^aThe donation is the sum of the atomic populations of Fe in the molecular orbitals whose main characters are the 5σ orbital of CO

^bThe total back donation is defined here as atomic populations of CO in active spaces (Fe 3d and 4s and CO 2π* orbitals) considered in CASSCF calculations

^cThe number in parentheses is the π back donation

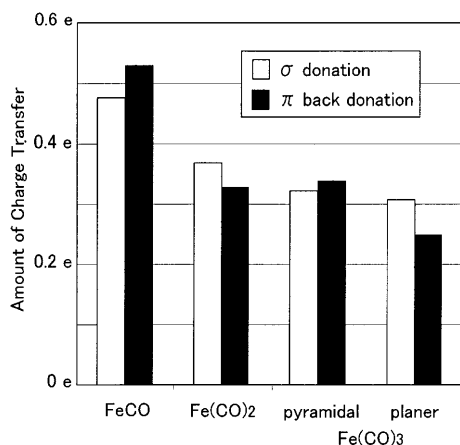


Fig. 2. Amount of donation and back donation per ligand

300 cm⁻¹. The Fe–C stretch decreases monotonously in going from FeCO to Fe(CO)₃; on the other hand, the totally symmetric C–O stretch has a maximum at Fe(CO)₂. This observation is consistent with the optimized C–O distance having a minimum at Fe(CO)₂.

3.2 Nature of bonding

The results of the population analysis of Fe(CO)_n (*n* = 1–3) are summarized in Table 3. We define the donation as a summation of the atomic populations of Fe in the molecular orbitals whose main characters are 5σ orbitals of CO ligands, namely, 10σ for FeCO, 8σ_g and 7σ_u for Fe(CO)₂, and 10*a*₁ and 9*e* for Fe(CO)₃. The total back donation is defined here as atomic populations of CO in active spaces considered in the CASSCF calculations. The total back donation consists of σ, π, and δ contributions. The π back donation shown in parentheses in Table 3 is the only dominant contribution to the total back donation because the σ and δ contributions are very small.

The donation and back donation mechanism is clearly seen for FeCO. The σ donation arises from the 5σ molecular orbital of CO to the unoccupied metal orbitals of σ symmetry, while the π back donation arises from the active Fe 3dπ orbitals to the empty antibonding orbital (2π*) of CO. The amount of back donation is 0.530, a value slightly

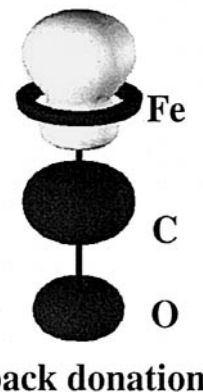
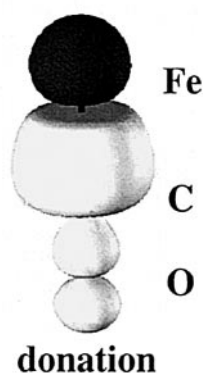


Fig. 3. Charge density difference map for FeCO. The charge density difference map for donation was obtained by subtracting the density of the 5σ molecular orbital of CO from the 10σ molecular orbital of FeCO and that for the back donation was obtained by subtracting the density of the 3d and 4s orbitals of Fe(³F) from that of the valence orbitals except 10σ. *Shadow* and *bright areas* indicate increases and decreases in densities, respectively

larger than the σ donation of 0.476; thus, the Fe atom bears a positive charge. This result is essentially the same as those of previous analyses [12, 18, 19] and supports the traditional donation and back donation mechanism [32].

For $\text{Fe}(\text{CO})_2$, the donation arises from two 5σ orbitals of CO ligands so that the amount of charge transfer increases by 0.260 compared to that for FeCO . On the other hand, the total back donation increases by only 0.125, and thus the net charge of the Fe atom changed from positive to negative.

For $\text{Fe}(\text{CO})_3$, the equilibrium geometry is now changed from a linear to a pyramidal form. The 5σ orbitals of three ligands belong to a_1 and degenerate e representations. The donation to Fe from these orbitals amounts to 0.965, while the total back donation to CO is 1.018; thus, the Fe atom again bears a small positive charge. A large $4p$ population of 0.65 is observed because of the formation of the d^2p hybrid orbital.

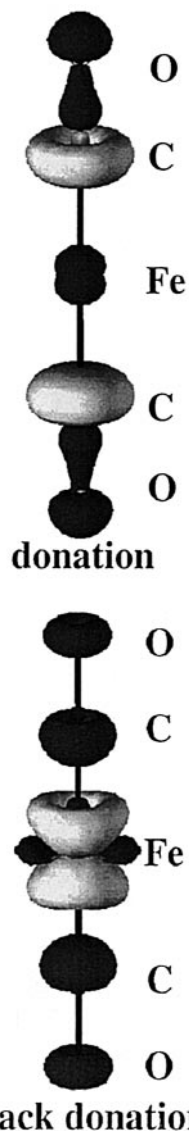


Fig. 4. Charge density difference map for $\text{Fe}(\text{CO})_2$. The charge density difference map for donation was obtained by subtracting the density of the 5σ molecular orbital of CO from those of the $8\sigma_g$ and $7\sigma_u$ molecular orbitals of $\text{Fe}(\text{CO})_2$ and that for the back donation was obtained by subtracting the density of the $3d$ and $4s$ orbitals of $\text{Fe}({}^3\text{F})$ from that of the valence orbitals except $8\sigma_g$ and $7\sigma_u$. Shadow and bright areas indicate increases and decreases in densities, respectively

The amount of donation from the 5σ orbital π back donation to the $2\pi^*$ orbitals increases linearly in going from FeCO to $\text{Fe}(\text{CO})_3$. The amount of donation and back donation per ligand is shown for three molecules in Fig. 2. The amount of charge transfer through σ donation per ligand decreases gradually. The trend corresponds to the change in the bond length of $\text{Fe}-\text{C}$, which increases from 1.795 to 1.925 Å. On the other hand, the amount of back donation to $2\pi^*$ has a minimum at $\text{Fe}(\text{CO})_2$, where we have the shortest $R(\text{C}-\text{O})$ distance. This can be explained by noting that the occupancy of the $2\pi^*$ antibonding orbital increases the $\text{C}-\text{O}$ length. When we compare the planar form of $\text{Fe}(\text{CO})_3$ with FeCO and $\text{Fe}(\text{CO})_2$, the amount of donation and back donation decreases monotonously as the number of ligands increases.

The charge-density differences for these molecules are shown in Figs. 3–5 charge-density differences were obtained by subtracting the density of fragment systems of Fe and CO from those of molecules at the equilibrium geometries. For all systems including $\text{Fe}(\text{CO})_3$, the donation and back donation occurs along the $\text{Fe}-\text{C}$ bond axis.

Summary

In this study, we carried out CASSCF–SDCI calculations for $\text{Fe}(\text{CO})_n$ ($n = 1-3$) in order to investigate the nature of bonding with respect to changes in the number

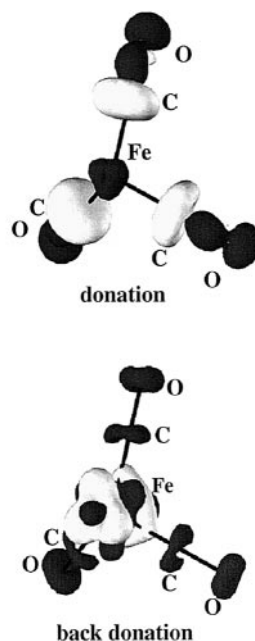


Fig. 5. Charge density difference map for $\text{Fe}(\text{CO})_3$. The charge density difference map for donation was obtained by subtracting the density of the 5σ molecular orbital of CO from those of the $10a_1$ and $9e$ molecular orbitals of $\text{Fe}(\text{CO})_3$ and that for the back donation was obtained by subtracting the density of the $3d$ and $4s$ orbitals of $\text{Fe}({}^3\text{F})$ from that of the valence orbitals except $10a_1$ and $9e$. Shadow and bright areas indicate increases and decreases in densities, respectively

of CO ligands. The calculated bond lengths of Fe—C were in reasonable agreement with the experimental values. Based on the Mulliken population analysis, the traditional donation and back donation mechanism is valid for FeCO to Fe(CO)₃. The donation from the 5σ orbitals per ligand decreases monotonously with changes in the number of ligands, thereby increasing the Fe—C length. On the other hand, the amount of back donation per ligand has a minimum at Fe(CO)₂, which reflects the shortest C—O length at Fe(CO)₂.

Acknowledgements. The authors would like to thank M. Yoshimine for provision of the ALCHEMY II software package. This work was supported by the Joint Studies Program (1999) of the Institute for Molecular Science (IMS), and some of the calculations were performed on the IBM RS/6000 PS2 cluster at the IMS.

References

1. Tanaka K, Sakaguchi K, Tanaka T (1997) *J Chem Phys* 106: 2118
2. Engelking PC, Lineberger WC (1979) *J Am Chem Soc* 101: 5569
3. Sunderlin LS, Wang D, Squires RR (1992) *J Am Chem Soc* 114: 2788
4. Sedar TA, Ouderkirk AJ, Weitz E (1986) *J Chem Phys* 85: 1977
5. Weitz E (1987) *J Phys Chem* 91: 3945
6. Ryther RJ, Weitz E (1991) *J Phys Chem* 95: 9841
7. Ryther RJ, Weitz E (1992) *J Phys Chem* 96: 2561
8. Villalta PW, Leopold DG (1993) *J Phys Chem* 98: 7730
9. Kasai Y, Obi K, Ohshima Y, Endo Y, Kawaguchi K (1995) *J Chem Phys* 103: 90
10. Tanaka K, Shirasaka M, Tanaka T (1997) *J Chem Phys* 106: 6820
11. (a) Tanaka K, Tachikawa Y, Tanaka T (1997) *Chem Phys Lett* 281: 285; (b) Tanaka K, Tachikawa Y, Sakaguchi K, Hikida T, Tanaka T (1999) *J Chem Phys* 111: 3970
12. Bauschlicher CW Jr, Bagus PS, Nelin CJ, Roos BO (1986) *J Chem Phys* 85: 354
13. Fournier R (1993) *J Chem Phys* 99: 1801
14. Ricca A, Bauschlicher CW Jr, Rosi M (1994) *J Phys Chem* 98: 9498
15. Castro M, Salahub DR, Fournier R (1994) *J Chem Phys* 100: 8233
16. Bauschlicher CW Jr (1994) *J Chem Phys* 100: 1215
17. Ricca A, Bauschlicher CW Jr (1995) *Theor Chim Acta* 92: 123
18. Adamo C, Leij F (1995) *J Chem Phys* 103: 10605
19. Adamo C, Leij F (1995) *Chem Phys Lett* 246: 463
20. Lüthi HP, Siegbahn PEM, Almlöf J (1985) *J Phys Chem* 89: 2156
21. Barnes LA, Bauschlicher CW Jr (1989) *J Chem Phys* 91: 314
22. Barnes LA, Rosi M, Bauschlicher CW Jr (1991) *J Chem Phys* 94: 2031
23. Bauschlicher CW Jr, Bagus PS (1984) *J Chem Phys* 81: 5889
24. González-Blanco O, Branchadell V (1999) *J Chem Phys* 110: 778
25. Koga T, Tatewaki H, Matsuyama H, Satoh Y *Theor Chem Acc* (in press)
26. Huzinaga S, Andzelm J, Klobukowski M, Radzio-Andzelm E, Sakai Y, Tatewaki H (1984) *Gaussian basis sets for molecular calculations*. Elsevier, Amsterdam
27. Noro T, Sekiya M, Koga T (1997) *Theor Chem Acc* 98: 25
28. Huber KP, Herzberg G (1979) *Constants of diatomic molecules* Van Nostrand Reinhold, New York
29. Lengsfeld BH III (1980) *J Chem Phys* 73: 382
30. (a) Liu B, Yoshimine M (1981) *J Chem Phys* 74: 612; (b) Lengsfeld BH III, Liu B (1981) *J Chem Phys* 75: 478
31. Shida N, Takeshita K, Yamamoto Y (1993) *Library Program at the Computing Center of Hokkaido University*
32. Cotton FA, Wilkinson G (1988) *Advanced inorganic chemistry*, 5th edn. Wiley-Interscience, New York
33. Poliakoff M (1974) *J Chem Soc Dalton Trans* 210
34. Poliakoff M, Turner JJ (1974) *J Chem Soc Dalton Trans* 2276